Front. Phys. 12(3), 128501 (2017)
DOI 10.1007/s11467-016-0649-3

RESEARCH ARTICLE

Thermal spin transfer torque in Fe|Ag|YIG multilayers

Hui-Min Tang[1,*], **Xing-Tao Jia**[2,*,†], **Shi-Zhuo Wang**[1]

[1] *Department of Physics, Beijing Normal University, Beijing 100875, China*
[2] *School of Physics and Electronic Information Engineering, Henan Polytechnic University, Jiaozuo 454000, China*
Corresponding author. E-mail: [†] *jiaxingtao@hpu.edu.cn*
Received September 29, 2016; accepted December 2, 2016

We investigated the thermal spin transfer effect in FM|NM|YIG multilayers using the first principles scattering theory. At room temperature, the spin Seebeck torque $T_{SSE} \sim 1.0$ μJ/(K·m^2) in an Ag|Fe|Ag|YIG multilayer, which is around 40% larger than that estimated from mixing conductance. The quantum effects such as interlayer exchange coupling between FM and YIG could be responsible for the enhancements. Based on the LLG equation, we predict that a temperature bias of ∼ 10 K can reverse the magnetic configurations, circularly, in a multilayer at room temperature.

Keywords spin Seebeck torque, spin transfer torque, YIG

PACS numbers 85.75.-d, 72.25.-b, 72.25.Mk

1 Introduction

Thermal spin transfer, which is the spin transfer created by thermoelectric effects, has attracted considerable attention in the field of "spin caloritronics" [1]. The large thermally driven spin transfer torque (STT) in all-metallic spin valves was first predicted by Hatami *et al.* [2], and it was experimentally found in a Co|Cu|Co nanowire by Yu *et al.* [3]. Subsequently, thermal torque has been predicted and found in spin valves [2–5], domain walls [6–9], magnetic tunnel junctions (MTJs) [10–13], and even normal-metal|ferromagnet (NM|FM) interfaces [14–18]. Among them, the NM|FM interface, especially NM|ferromagnetic insulator (NM|FI) interface, has the potential to serve as the basic unit in spin caloritronics.

The thermal torque at NM|FI interfaces is considered to be interesting for its pure spin-driven process. Two mechanisms are proposed for the interface [18]: the first one is the local effect of torque on the magnetization via magnon-magnon scattering driven by a spin Seebeck effect (SSE) [5], the other one is the nonlocal effect of torque on the magnetization via absorption of spin current generated by misaligned magnetization. These mechanisms are based on SSE, which is driven by the temperature difference between the magnon of FM(FI) and the lattice of NM. This difference is large in spin valves, in which the thermal torque is carried by the spin polarizing electrons and driven by the temperature difference between the electrons in FMs. To classify the two types of thermal torques, the torque from the SSE is named as spin Seebeck torque (T_{SSE}) and that from the nonlocal electrons as thermal spin pumping torque (T_{SP}). The latter can be calculated using the spin pumping theory [19], which is based on the scattering theory. Recent experiments revealed that a small temperature bias of 1 K can build a spin torque of the order 1.0 μJ/(K·m^2) [20, 21], which is several times larger than that [10, 22] in ultrathin MgO-based magnetic tunnel junctions (MTJs).

When a ferromagnet is attached to the NM|FI interface, forming a FM|NM|FI multilayer, the spin current pumped out of the FI/FM generates a torque on the FM/FI. Both SEE and anomalous Nernst effect (ANE) are present under the temperature bias. A recent experiment in Co|Cu|YIG demonstrates that SSE dominates over ANE [23]. As the spin torque overcomes the damping torque, a stable magnetic oscillation or magnetic switching would be generated. For an NM|FI interface, the spin mixing conductance is a good parameter to estimate the power required to generate a spin torque [20]. Through experiments, it is easier to measure the spin torque than the spin mixing conductance; therefore, it is convenient to derive the spin mixing conductance from the measured spin torque.

*These authors contributed equally to this study and share first authorship.

Here, we study the thermal torque in Ag|Fe|Ag|YIG multilayers using first principles. Owing to the ultralow intrinsic magnetic damping α_0, Yttrium iron garnet ($Y_3Fe_5O_{12}$) is a promising material for spin-wave applications [5, 24–32]. A low magnetic damping [33–37] $\sim 10^{-4}$ was reported in YIG thin films, which is close to that in bulk YIG. In our calculations, an enhanced magnetic damping $\alpha \sim 0.059$ from interface scattering and $T_{SSE} \sim 1.0$ μJ/(K·m^2) at 300 K were estimated. Based on the Landau–Lifshitz–Gilbert (LLG) equation [38], we predict that a temperature bias of ~ 10 K across the sandwiched NM is sufficient to reverse the magnetic configurations circularly in a multilayer at room temperature.

This article is organized as follows: In Section 2, we introduce the spin Seebeck torque induced by magnetic precession. In Section 3, we present our results on Ag|Fe|Ag|YIG multilayers, where two methods are used to estimate the spin Seebeck torque from the spin mixing conductance and the magnetic damping parameter. The study is summarized in Section 4.

2 Enhanced magnetic damping and spin Seebeck torque

In this section, we explain the use of scattering theory to calculate the magnetic damping and spin Seebeck torque in NM|FM|NM|FI|NM multilayers, as shown in Fig. 1. The same NM is used for both the right and left leads, and when the FI is sufficiently thick, the right lead shows less effect on the spin transport. Magnetization dynamics in the FI is usually described by the phenomenological LLG equation [40]:

$$\dot{\boldsymbol{m}}(\boldsymbol{r},t) = -\gamma \boldsymbol{m}(\boldsymbol{r},t) \times [\boldsymbol{H}_{eff}(\boldsymbol{r},t) + \boldsymbol{h}(\boldsymbol{r},t)] + \boldsymbol{m}(\boldsymbol{r},t) \times \int \mathrm{d}\boldsymbol{r}' [\widetilde{\alpha}[\boldsymbol{m}](\boldsymbol{r},\boldsymbol{r}') \dot{\boldsymbol{m}}(\boldsymbol{r}',t)], \quad (1)$$

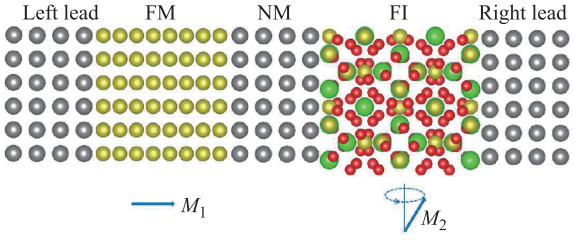

Fig. 1 Schematic structure of Ag|Fe|Ag|YIG|Ag. The red and green atoms in YIG denote the O and Y atoms, respectively. We consider the magnetization ($\boldsymbol{M}_2$) of YIG precessing around the quantum z axis, and the magnetization ($\boldsymbol{M}_1$) of FM sets free in the x−z plane. We assume temperature difference exited only at YIG|Ag and Fe|Ag interfaces [39], and ignore the spin transfer from Fe/YIG to left/right lead.

where $\dot{\boldsymbol{m}}(\boldsymbol{r},t) = \partial \boldsymbol{m}(\boldsymbol{r},t)/\partial t$, $\boldsymbol{m}(\boldsymbol{r},t)$ is the unit vector of the magnetization texture at position $\boldsymbol{r}$ and time t, $\boldsymbol{H}_{eff}$ and $\boldsymbol{h}$ are the effective magnetic field and random magnetic field [5] due to the magnetization, respectively, and $\gamma = g\mu_B/\hbar$ is the gyromagnetic ratio. The magnetic damping $\widetilde{\alpha}$ is a 3×3 tensor, which depends on the orientation of magnetization.

The time derivative of the magnetic energy E, obtained from the above equation is [40]

$$\dot{E} = -M_s \int \mathrm{d}\boldsymbol{r} [\dot{\boldsymbol{m}}(\boldsymbol{r},t) \cdot \boldsymbol{H}_{eff}(\boldsymbol{r},t)] = \frac{M_s}{\gamma} \int \mathrm{d}\boldsymbol{r} \int \mathrm{d}\boldsymbol{r}' \dot{\boldsymbol{m}}(\boldsymbol{r}) \cdot \widetilde{\alpha}[\boldsymbol{m}](\boldsymbol{r},\boldsymbol{r}') \cdot \dot{\boldsymbol{m}}(\boldsymbol{r}'), \quad (2)$$

where M_s is the saturation magnetization. Therefore, the magnetic damping is directly related to the energy pumping process. The rate of energy loss in the scattering region in terms of the scattering matrix [41, 42] at finite temperatures is given by

$$\dot{E} = \frac{\hbar}{4\pi} \int \mathrm{d}\epsilon \left(\frac{\partial f}{\partial \epsilon}\right) \mathrm{Tr} \left[\frac{\partial S(\epsilon,t)}{\partial t} \frac{\partial S^\dagger(\epsilon,t)}{\partial t}\right], \quad (3)$$

where $S = [r, t'; t, r']$ is the scattering matrix with transmission/reflection matrices (t/r) for the Bloch waves incident from the left (without prime) and right (with prime) leads. Comparing Eqs. (2) and (3), we obtain the magnetic damping tensor expressed by the scattering matrix:

$$\widetilde{\alpha}_{ij} = \frac{\gamma\hbar}{4\pi M_s V} \mathrm{Tr} \left[\frac{\partial S(\epsilon)}{\partial m_i} \frac{\partial S^\dagger(\epsilon)}{\partial m_j}\right], \quad (4)$$

where V is the volume of magnetization with section area A and thickness d_f. For the FI|NM interface, neglecting the spin-orbit coupling, the magnetic damping tensor can be reduced to a magnetic damping parameter $\alpha = \gamma\hbar g_r/(4\pi M_s V)$, where g_r is the real part of the spin-mixing conductance [41, 42].

At finite temperatures, α includes the value of temperature via two parameters: the Fermi–Dirac distribution $f = \{\exp[(\epsilon - \epsilon_F)/(K_B T)] + 1\}^{-1}$, and the temperature dependent magnetic coherence volume [20] $V_a = \frac{2}{3\xi(5/2)} (\frac{4\pi D}{k_B T})^{3/2}$, where D is the the spin-wave stiffness constant and ξ is the Riemann Zeta function. The thermal magnetic damping parameter can be expressed as

$$\widetilde{\alpha}^T_{ij} = \frac{\gamma\hbar}{4\pi M_s V_a} \int \mathrm{d}\epsilon \left(-\frac{\partial f}{\partial \epsilon}\right) \mathrm{Tr} \left[\frac{\partial S(\epsilon)}{\partial m_i} \frac{\partial S^\dagger(\epsilon)}{\partial m_j}\right]. \quad (5)$$

At zero temperature, V_a is reduced to V, and $-\partial f/\partial\epsilon$ is reduced to $\delta(\epsilon - \epsilon_F)$ at the Fermi energy ϵ_F.

When there is a temperature difference between two magnetic layers, as in the FM|NM|FI multilayer shown in Fig. 1, a thermal spin current arising from the thermally induced spin fluctuation is generated and it flows from

the high-temperature layer $\boldsymbol{M_2}$ across the NM [5]

$$\langle I_s \rangle = 2\alpha^T k_B \Delta T. \quad (6)$$

The spin current is polarized along the equilibrium magnetization $\boldsymbol{M_2}$. The thermally induced spin current $\langle I_s \rangle$ enters the magnetic layer $\boldsymbol{M_1}$ and generates a spin-transfer torque. When the working frequencies of FM and FI are different, there is a weak interaction between the spin currents being pumped from FI and FM. Therefore, the total spin current in the sandwiched NM would be the sum of the spin currents from both FI and FM. Considering that the spin current pumping out of the NM|FI interface is fully absorbed by the FM, the spin torque exerted on $\boldsymbol{M}_1$ is

$$\begin{aligned} \boldsymbol{T}_{SSE} &= \langle I_s \rangle \boldsymbol{M}_1 \times (\boldsymbol{M}_2 \times \boldsymbol{M}_1) \\ &= 2\alpha^T k_B \Delta T [\boldsymbol{M}_1 \times (\boldsymbol{M}_2 \times \boldsymbol{M}_1)], \end{aligned} \quad (7)$$

which is referred to as the spin Seebeck torque. When the quantum effect in the sandwiched NM is negligible, the total spin Seebeck torque is reduced to [5] $\boldsymbol{T}_{SSE} = \frac{\gamma \hbar g_r}{2\pi M_s V_a} k_B \Delta T [\boldsymbol{M}_1 \times (\boldsymbol{M}_2 \times \boldsymbol{M}_1)]$.

3 Spin Seebeck torque in Fe|Ag|YIG multilayers

Here, we study the enhanced magnetic damping and thermal torque in Ag|Fe|Ag|YIG multilayers, as shown in Fig. 1. We use a 3×3 lateral supercell for the fcc Ag, so that it matches the cubic YIG unit cell. The electronic structure of the YIG is calculated using a tight-binding linear-muffin-tin-orbital (TB-LMTO) code in the augmented spherical wave approximation, as implemented in the Stuttgart code [43–45] using the generalized gradient approximation (GGA) to the local density approximation (LDA); and the bulky potentials are added into a wave-function matching (WFM) transport package [46]. During transport calculations, we consider the particle current along the (010) material growth direction, and a 40×40 k-mesh in the two-dimensional Brillouin zone (2d-BZ) is used to ensure good transport convergence. Additional numerical details about the electronic structure and transport calculations can be found in the reference [47].

First, let us consider the T_{SP} in the Ag|Fe|Ag|YIG multilayers. $\boldsymbol{T}_{SP} = -M_s V[\boldsymbol{m} \times \mathrm{Tr}(\boldsymbol{Q}^L - \boldsymbol{Q}^R)V_b]$ can be estimated from the scattering matrix [48], where $Q_j^{L/R} = \frac{\mathrm{i}e}{4\pi M_s V} \sum_{L/R} S\partial_{m_j} S^\dagger + H.c$ summarize the modes of the left/right (L/R) lead and $V_b = (\mu_R - \mu_L)/e$ is the voltage bias estimated from the local chemical potentials $\mu_{L/R}$. In the case of a thicker YIG, the right-going electrons would be reflected to left completely, and no pure electrons will penetrate through the YIG. Here, a 2.0 nm YIG was used for the calculations, and the transmission was on the order of 10^{-10}. Consequently, the in-plane STT from Fe/YIG to YIG/Fe would be zero for the non-local nature. However, the out-of-plane STT is non-zero, as shown in the inset of Fig. 2(a), which is due to the local exchange interaction between Fe and YIG. From the energy dependent STT, we obtain the T_{SP} [10]. A T_{SP} of 71 nJ/(K·m^2) was found in Ag|Fe(16)|Ag(16)|YIG at 300 K, where the numbers in brackets indicate the thickness of the atomic layers. However, when Pt is considered as a separate metal, a large T_{SP} of -680 nJ/(K·m^2) is observed, as listed in Table 1, which is even larger than that in Fe|MgO(3)|Fe MTJs [10]. The large difference in T_{SP} results from the large symmetric difference in energy-dependent STT as shown in the inset of Fig. 2(a), which is related to the large difference in the symmetry of the density of states of the sandwiched NM at Fermi energy in the two multilayers, as shown in the Fig. 2(b).

Though the out-of-plane spin torque shows less effect on the magnetic switching [22], it can change the resistance in the structure via inverse spin Hall effect (ISHE). The out-of-plane T_{SP} originates from a spin current along the y axis with a spin polarization in the x direction. When the spin current is absorbed by the sandwiched NM via spin-orbital coupling, it would produce an electron flow along the z axis via ISHE. Therefore, the lateral resistance can be varied in the presence

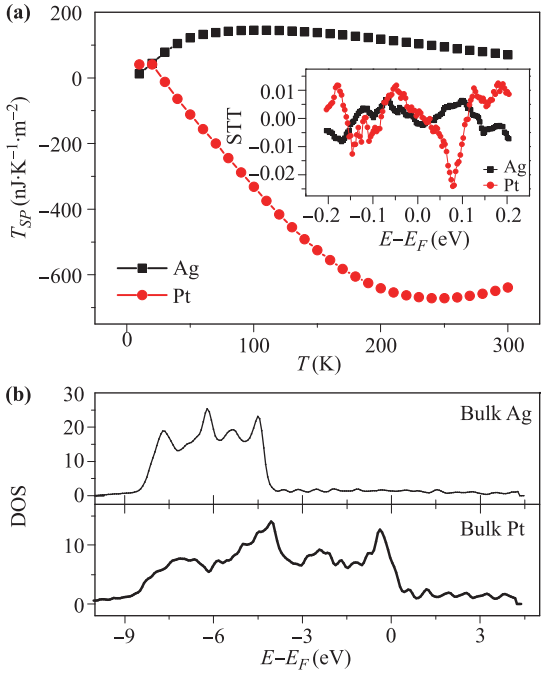

Fig. 2 **(a)** Temperature dependence of the out-of-plane T_{SP} in Ag|Fe(16)|Ag(16)|YIG|Ag and Pt|Fe(16)|Ag(16)|YIG|Pt from first principle scattering theory calculation. inset: energy dependence of the out-of-plane STT. **(b)** Density of states of the bulk Ag and Pt.

Table 1 Thermal torque in NM|Fe(16)|NM(16)|YIG (NM = Ag and Pt) at 300 K. ΔT_{SW} is calculated according to LLG equations [38] with saturation magnetization $M_S = 1$ T, uniaxial anisotropy field $\mu_0 H_K = 25$ mT, dimensionless planar anisotropy $h_p = K_P/K = 20$ is the ratio of easy-plane anisotropy energy K_P to uniaxial anisotropy energy $K = (1/2)M_S H_K$, The thickness of Fe region is consider as 2.0 nm, and taking intrinsic magnetic damping coefficient of 0.01, and the enhanced magnetic damping coefficient of 0.0073/0.007 for Ag/Pt spacer.

Spacer	α^T	T_{SP} (nJ·K^{-1}·m^{-2})	T_{SSE} (nJ·K^{-1}·m^2)	ΔT_{SW} (K)
Ag	0.059	71	1075	12
Pt	0.055	−680	930	14

of thermal pumping torque.

The spin Seebeck torque can be considered as a local effect, which is directly related to the thermal magnetic damping α^T. Figure 3 shows α^T and T_{SSE} as functions of temperature in the Ag|Fe(16)|Ag(16)|YIG multilayer. At high temperatures, both α^T and T_{SSE} are proportional to $T^{3/2}$, and a deviation is observed at low temperatures. The temperature dependence is consistent with that estimated from Eq. (5). Therein, for $\partial_{m_i} S \partial_{m_j} S^\dagger \sim \lambda_c^2$, where $\lambda_c = V_a^{1/3}$ is the magnetic coherence length, we obtain $\lambda_c \sim T^{-1/2}$; consequently, $\alpha_{ij} \sim T^{1/2}$ and $T_{SSE} \sim T^{3/2}$. That is, T_{sse} can decrease to one-thirty, when the temperature decreases one order. We found that $\alpha^T \sim 0.059$ and $T_{SSE} \sim 1075$ nJ/(K·m^2) in Ag|Fe(16)|Ag(16)|YIG at 300 K, considering $\lambda_c \sim 1.3$ nm and taking [5] $D = 1.55 \times 10^{-38}$ J·m^2. When Pt is the separate metal, $\alpha^T \sim 0.055$ and $T_{SSE} \sim 929$ nJ/(K·m^2), as listed in Table 1. Comparatively, T_{SSE} would dominate over T_{SP} in both the spin valves. By including the thermal torque in the LLG equation [38], we obtain a temperature gradient $\Delta T_{SW} = 12/14$ K that is sufficient to switch the magnetization in Fe between antiparallel (AP) and parallel (P) configurations in the NM|Fe(16)|NM(16)|YIG multilayer with Ag/Pt spacer, as listed in Table 1, which is of the same order as that in the MgO-based MTJs [10, 19, 22].

The origin of large α^T and T_{SSE} can be found from the inset of Fig. 3, which shows the energy-dependent α. We find that: i) $\alpha(E)$ is dominated by the diagonal part, and the off-diagonal part is several times smaller than the diagonal part. ii) α_{xx} is considerable larger than both α_{yy} and α_{zz}, indicating that the magnetic damping is anisotropic. The break in rotational symmetry is related to the structural symmetry and the existence of quantum states in the spin valves. α_{xx}, which corresponds to M_2 rotates slightly towards x, and this rotation pumps spin current into M_1 with a spin polarization along the y-axis. The pumped spin current can be absorbed by M_1, which is along the x-axis, leading to an enhancement of the magnetic damping. When M_2 rotates towards the y-axis, the pumped spin current is polarized along the x direction, and is hardly absorbed by M_1, leading to small magnetic damping. As a result, the damping component becomes asymmetric.

When the sandwiched NM is sufficiently thick, the contribution from quantum effects would be very weak, and the magnetic damping α would be dominated by the spin mixing conductance at the NM|FI interface, as spin flip in the sandwiched NM is negligible. In Fig. 3, the α^T and T_{SSE} estimated from the spin mixing conductance are also given. Both α_T and T_{SSE} estimated from the spin mixing conductance are about 40% smaller than that estimated from the calculations. This indicates that the quantum effect in multilayers cannot be ignored.

Interlayer exchange coupling is usually observed in multilayers. The effects of interlayer exchange coupling can be observed from Fig. 4, which shows the thickness dependence of α on the sandwiched NM in

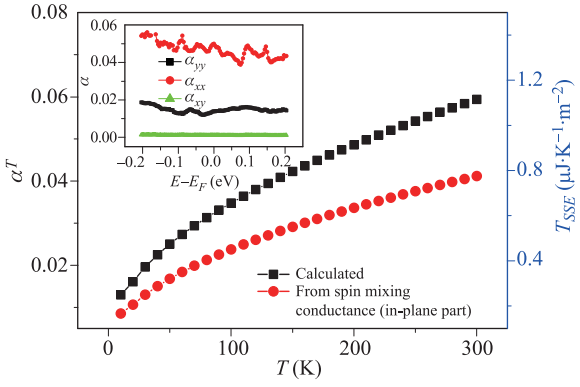

Fig. 3 α^T and T_{SSE} in Ag|Fe(16)|Ag(16)|YIG|Ag from first principle scattering theory calculations and that estimated from spin mixing conductance. Inset: Energy-dependent magnetic damping.

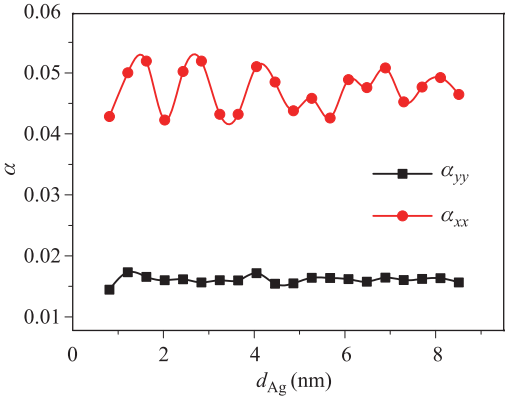

Fig. 4 α in the clean Ag|Fe|Ag|YIG multilayers as function of the thickness of the sandwiched Ag.

Ag|Fe(16)|Ag(x)|YIG multilayers. A slowly damped oscillation is observed in α_{xx}, as the function of Ag thickness varied from 1 to 9 nm. As the thickness of the sandwiched Ag is below 5 nm, the oscillation period is approximately 1.3 nm, which is close to those in FM|Ag|FM and FM|Cu|FM [49]. This result indicates that spin pumping is affected by the interlayer exchange coupling in the Ag spacer. At the same time, the oscillatory behavior in α, also exists in T_{SSE}, thus providing another method for measuring the interlayer exchange coupling through the calculation of spin torque.

4 Summary

We investigated the enhanced magnetic damping and thermal spin transfer effects in NM|Fe|NM|YIG multilayer from first principles studies. The spin Seebeck torque T_{SSE} of 1075/929 nJ/(K·m^2) is found in the multilayers Ag/Pt spacer at 300 K, which is considerably larger than the thermal spin pumping torque T_{SP} of $71/-634$ nJ/(K·m^2). Based on the LLG equation, we estimated that a temperature bias of ~ 10 K across the sandwiched NM would be sufficient to reverse the magnetic configurations circularly in a multilayer at room temperature. Moreover, T_{SSE} estimated on the basis of first-principles, is considerably larger than that estimated from spin mixing conductance, indicating that the quantum effect in spin valves cannot be ignored. It is easy to measure the spin torque experimentally, therefore, quantum effects such as interlayer exchange, can be estimated from the spin torque in multilayers.

Acknowledgements We thank K.X. at BNU for the supports in the calculations, and gratefully acknowledge financial support from the National Natural Science Foundation of China under Grant Nos. 11274094 and 11174037. X.J. also acknowledges financial support from Henan Polytechnic University with Grant Nos. B2012-021 and T2016-2.

References

1. G. E. W. Bauer, E. Saitoh, and B. J. van Wees, Spin caloritronics, *Nat. Mater.* 11(5), 391 (2012)
2. M. Hatami, G. E. W. Bauer, Q. Zhang, and P. J. Kelly, Thermal spin-transfer torque in magnetoelectronic devices, *Phys. Rev. Lett.* 99(6), 066603 (2007)
3. H. Yu, S. Granville, D. P. Yu, and J. Ph. Ansermet, Evidence for thermal spin-transfer torque, *Phys. Rev. Lett.* 104(14), 146601 (2010)
4. M. Hatami, G. E. W. Bauer, Q. Zhang, and P. J. Kelly, Thermoelectric effects in magnetic nanostructures, *Phys. Rev. B* 79(17), 174426 (2009)
5. J. Xiao, G. E. W. Bauer, K. C. Uchida, E. Saitoh, and S. Maekawa, Theory of magnon-driven spin Seebeck effect, *Phys. Rev. B* 81(21), 214418 (2010)
6. Z. Yuan, S. Wang, and K. Xia, Thermal spin-transfer torques on magnetic domain walls, *Solid State Commun.* 150(11–12), 548 (2010)
7. A. A. Kovalev and Y. Tserkovnyak, Thermoelectric spin transfer in textured magnets, *Phys. Rev. B* 80(10), 100408 (2009)
8. G. E. W. Bauer, S. Bretzel, A. Brataas, and Y. Tserkovnyak, Nanoscale magnetic heat pumps and engines, *Phys. Rev. B* 81(2), 024427 (2010)
9. A. A. Kovalev and Y. Tserkovnyak, Magnetocaloritronic nanomachines, *Solid State Commun.* 150(11–12), 500 (2010)
10. X. Jia, K. Xia, and G. E. W. Bauer, Thermal spin transfer in Fe-MgO-Fe tunnel junctions, *Phys. Rev. Lett.* 107(17), 176603 (2011)
11. X. Jia and K. Xia, Thermal electric effects in Fe-GaAs-Fe tunnel junctions, *AIP Adv.* 2(4), 041411 (2012)
12. S. Z. Wang, K. Xia, and G. E. W. Bauer, Thermoelectricity and disorder of FeCo/MgO/FeCo magnetic tunnel junctions, *Phys. Rev. B* 90(22), 224406 (2014)
13. X. Jia and K. Xia, Electric and thermo spin transfer torques in Fe/Vacuum/Fe tunnel junction, *Front. Phys.* 9(6), 768 (2014)
14. J. C. Slonczewski, Initiation of spin-transfer torque by thermal transport from magnons, *Phys. Rev. B* 82(5), 054403 (2010)
15. E. Padrón-Hernández, A. Azevedo, and S. M. Rezende, Amplification of spin waves by thermal spin-transfer torque, *Phys. Rev. Lett.* 107(19), 197203 (2011)
16. M. B. Jungfleisch, T. An, K. Ando, Y. Kajiwara, K. Uchida, V. I. Vasyuchka, A. V. Chumak, A. A. Serga, E. Saitoh, and B. Hillebrands, Heat-induced damping modification in yttrium iron garnet/platinum heterostructures, *Appl. Phys. Lett.* 102(6), 062417 (2013)
17. L. Lu, Y. Sun, M. Jantz, and M. Wu, Control of ferromagnetic relaxation in magnetic thin films through thermally induced interfacial spin transfer, *Phys. Rev. Lett.* 108(25), 257202 (2012)
18. S. A. Bender and Y. Tserkovnyak, Thermally driven spin torques in layered magnetic insulators, *Phys. Rev. B* 93(6), 064418 (2016)
19. X. Jia, S. Wang, and M. H. Qin, Enhanced thermal spin transfer in MgO-based double-barrier tunnel junctions, *New J. Phys.* 18(6), 063012 (2016)
20. M. Weiler, M. Althammer, M. Schreier, J. Lotze, M. Pernpeintner, S. Meyer, H. Huebl, R. Gross, A. Kamra, J. Xiao, Y. T. Chen, H. Jiao, G. E. W. Bauer, and S. T. B. Goennenwein, Experimental test of the spin mixing interface conductivity concept, *Phys. Rev. Lett.* 111(17), 176601 (2013)

21. A. Pushp, T. Phung, C. T. Rettner, B. Hughes, S. Yang, and S. S. P. Parkin, Giant thermal spin-torque assisted magnetic tunnel junction switching, *Proc. Natl. Acad. Sci. USA* 112(21), 6585 (2015)
22. P. Ogrodnik, G. E. W. Bauer, and K. Xia, Thermally induced dynamics in ultrathin magnetic tunnel junctions, *Phys. Rev. B* 88(2), 024406 (2013)
23. D. Tian, Y. Li, D. Qu, X. Jin, and C. L. Chien, Separation of spin Seebeck effect and anomalous Nernst effect in Co/Cu/YIG, *Appl. Phys. Lett.* 106(21), 212407 (2015)
24. Y. Kajiwara, K. Harii, S. Takahashi, J. Ohe, K. Uchida, M. Mizuguchi, H. Umezawa, H. Kawai, K. Ando, K. Takanashi, S. Maekawa, and E. Saitoh, Transmission of electrical signals by spin-wave interconversion in a magnetic insulator, *Nature* 464(7286), 262 (2010)
25. K. Uchida, J. Xiao, H. Adachi, J. Ohe, S. Takahashi, J. Ieda, T. Ota, Y. Kajiwara, H. Umezawa, H. Kawai, G. E. W. Bauer, S. Maekawa, and E. Saitoh, Spin Seebeck insulator, *Nat. Mater.* 9(11), 894 (2010)
26. C. W. Sandweg, Y. Kajiwara, A. V. Chumak, A. A. Serga, V. I. Vasyuchka, M. B. Jungfleisch, E. Saitoh, and B. Hillebrands, Spin pumping by parametrically excited exchange magnons, *Phys. Rev. Lett.* 106(21), 216601 (2011)
27. B. Heinrich, C. Burrowes, E. Montoya, B. Kardasz, E. Girt, Y. Y. Song, Y. Sun, and M. Z. Wu, Spin pumping at the magnetic insulator (YIG)/normal metal (Au) interfaces, *Phys. Rev. Lett.* 107(6), 066604 (2011)
28. H. Kurebayashi, O. Dzyapko, V. E. Demidov, D. Fang, A. J. Ferguson, and S. O. Demokritov, Controlled enhancement of spin-current emission by three-magnon splitting, *Nat. Mater.* 10(9), 660 (2011)
29. E. Padrón-Hernández, A. Azevedo, and S. M. Rezende, Amplification of spin waves by thermal spin-transfer torque, *Phys. Rev. Lett.* 107(19), 197203 (2011)
30. V. Castel, N. Vlietstra, J. Ben Youssef, and B. J. van Wees, Platinum thickness dependence of the inverse spin-Hall voltage from spin pumping in a hybrid yttrium iron garnet/platinum system, *Appl. Phys. Lett.* 101(13), 132414 (2012)
31. S. Y. Huang, X. Fan, D. Qu, Y. P. Chen, W. G. Wang, J. Wu, T. Y. Chen, J. Q. Xiao, and C. L. Chien, Transport magnetic proximity effects in platinum, *Phys. Rev. Lett.* 109(10), 107204 (2012)
32. H. Nakayama, M. Althammer, Y. T. Chen, K. Uchida, Y. Kajiwara, D. Kikuchi, T. Ohtani, S. Geprägs, M. Opel, S. Takahashi, R. Gross, G. E. W. Bauer, S. T. B. Goennenwein, and E. Saitoh, Spin Hall magnetoresistance induced by a nonequilibrium proximity effect, *Phys. Rev. Lett.* 110(20), 206601 (2013)
33. Y. Sun, Y. Y. Song, H. Chang, M. Kabatek, M. Jantz, W. Schneider, M. Wu, H. Schultheiss, and A. Hoffmann, Growth and ferromagnetic resonance properties of nanometer-thick yttrium iron garnet films, *Appl. Phys. Lett.* 101(15), 152405 (2012)
34. O. d'Allivy Kelly, A. Anane, R. Bernard, J. Ben Youssef, C. Hahn, A. H. Molpeceres, C. Carretero, E. Jacquet, C. Deranlot, P. Bortolotti, R. Lebourgeois, J. C. Mage, G. de Loubens, O. Klein, V. Cros, and A. Fert, Inverse spin Hall effect in nanometer-thick yttrium iron garnet/Pt system, *Appl. Phys. Lett.* 103(8), 082408 (2013)
35. T. Liu, H. Chang, V. Vlaminck, Y. Sun, M. Kabatek, A. Hoffmann, L. Deng, and M. Wu, Ferromagnetic resonance of sputtered yttrium iron garnet nanometer films, *J. Appl. Phys.* 115(17), 17A501 (2014)
36. H. L. Wang, C. H. Du, Y. Pu, R. Adur, P. C. Hammel, and F. Y. Yang, Scaling of spin hall angle in 3d, 4d, and 5d metals from $Y_3Fe_5O_{12}$/Metal spin pumping, *Phys. Rev. Lett.* 112(19), 197201 (2014)
37. H. C. Chang, P. Li, W. Zhang, T. Liu, A. Hoffmann, L. J. Deng, and M. Z. Wu, Nanometer-thick yttrium iron garnet films with extremely low damping, *IEEE Magn. Lett.* 5, 1 (2014)
38. J. Z. Sun, Spin-current interaction with a monodomain magnetic body: A model study, *Phys. Rev. B* 62(1), 570 (2000)
39. J. Zhang, M. Bachman, M. Czerner, and C. Heiliger, Thermal transport and nonequilibrium temperature drop across a magnetic tunnel junction, *Phys. Rev. Lett.* 115(3), 037203 (2015)
40. A. Brataas, Y. Tserkovnyak, and G. E. W. Bauer, Magnetization dissipation in ferromagnets from scattering theory, *Phys. Rev. B* 84(5), 054416 (2011)
41. Y. Tserkovnyak, A. Brataas, and G. E. W. Bauer, Spin pumping and magnetization dynamics in metallic multilayers, *Phys. Rev. B* 66(22), 224403 (2002)
42. Y. Tserkovnyak, A. Brataas, and G. E. W. Bauer, Enhanced Gilbert damping in thin ferromagnetic films, *Phys. Rev. Lett.* 88(11), 117601 (2002)
43. O. Gunnarsson, O. Jepsen, and O. K. Andersen, Self-consistent impurity calculations in the atomic-spheres approximation, *Phys. Rev. B* 27(12), 7144 (1983)
44. O. K. Andersen and O. Jepsen, Explicit, first-principles tight-binding theory, *Phys. Rev. Lett.* 53(27), 2571 (1984)
45. O. Jepsen, O. K. Andersen, and D. Glötzel, Highlights of Condensed Matter Theory, Amsterdam: North-Holland, 1985
46. S. Wang, Y. Xu, and K. Xia, First-principles study of spin-transfer torques in layered systems with non-collinear magnetization, *Phys. Rev. B* 77(18), 184430 (2008)
47. X. Jia, K. Liu, K. Xia, and G. E. W. Bauer, Spin transfer torque on magnetic insulators, *EPL* 96(1), 17005 (2011)
48. K. M. D. Hals, A. Brataas, and Y. Tserkovnyak, Scattering theory of charge-current induced magnetization dynamics, *EPL* 90(4), 47002 (2010)
49. P. Bruno and C. Chappert, Oscillatory coupling between ferromagnetic layers separated by a nonmagnetic metal spacer, *Phys. Rev. Lett.* 67(12), 1602 (1991)